

Analytically-based solutions for linear sloshing
Odd M. Faltinsen¹, Alexander Timokha
Dept. Marine Technology & Centre for Ships and Ocean Structures,
Norwegian University of Science and Technology,
NO-7491, Trondheim, Norway; odd.faltinsen@ntnu.no

Analytical approximations of linear sloshing with potential flow of an incompressible liquid are considered. The presented cases involve the Rayleigh quotient variational formulation, analytical continuation and asymptotic methods in the eigenvalue problem as well as linear modal theory for the forced motion problem.

1. Rayleigh quotient and variational equation. The original spectral boundary problem on a natural sloshing frequency σ and mode φ is due to the Rayleigh quotient associated with the extrema (local minima) of the functional

$$K_{Q_0, \Sigma_0}(\varphi) = \kappa = \frac{\sigma^2}{g} = \frac{\int_{Q_0} (\nabla \varphi)^2 dQ}{\int_{\Sigma_0} \varphi^2 dS} \quad \text{for} \quad \int_{\Sigma_0} \varphi dS = 0. \quad (1)$$

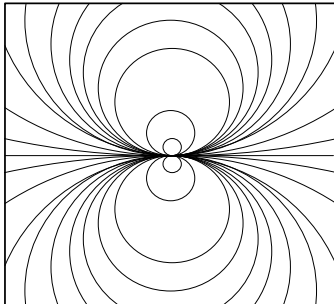
Here Σ_0 and Q_0 are the mean free surface and liquid domain, respectively, and $\varphi \cos(\sigma t)$ is a velocity potential. The lowest natural frequency σ_1 gives the absolute minimum of (1) with φ_1 . Using theorems on the quotient (Feshchenko et al., 1969; Faltinsen & Timokha, 2009) makes it possible to get upper and lower bounds of the natural frequencies and modes. However, the difference between the upper and lower bounds may in some cases be too large to provide a satisfactory estimate.

The necessary extrema condition for (1) deduces the variational equation for the natural modes φ_m

$$\int_{Q_0} (\nabla \varphi_m \cdot \nabla(\delta\varphi)) dQ - \kappa_m \int_{\Sigma_0} \varphi_m \delta\varphi dS = 0 \quad (2)$$

to be fulfilled for all the smooth functions $\delta\varphi$. The Laplace equation and all the boundary conditions are then *natural*, i.e. follow from (2). This means that the test functions used in minimizing eq. (1) for $m = 1$ need only to satisfy liquid volume conservation. Higher modes must be orthogonal to lower modes.

Table 1. Non-dimensional lowest eigenvalue $\kappa_1 R_0 = \sigma_1^2 R_0 / g$ for a 2D circular tank and $\kappa_{1,1} R_0 = \sigma_{1,1}^2 R_0 / g$ for a spherical tank as a function of the ratio between filling depth h and radius R_0 (McIver, 1989). Estimates of $\kappa_1 R_0$ and $\kappa_{1,1} R_0$ based on variational formulation are also given together with vertical position a of dipole singularity above mean free surface.

Stream lines of the dipole-like solution for 2D case	$\frac{h}{R_0}$	2D circular tank			Spherical tank		
		$\kappa_1 R_0$	With test function		$\kappa_{1,1} R_0$	With test function	
			$\kappa_1 R_0$	a / R_0		$\kappa_{1,1} R_0$	a / R_0
	0.2	1.04385	1.044012	1.836	1.07232	1.07233	2.7328
	0.4	1.09698	1.09778	1.673	1.15826	1.15833	2.465
	0.6	1.16268	1.164845	1.511	1.26251	1.2628	2.1953
	0.8	1.24606	1.25077	1.348	1.39239	1.3933	1.9245
	1.0	1.35573	1.36488	1.185	1.56016	1.5625	1.6527
	1.2	1.50751	1.524338	1.018	1.78818	1.794	1.3791
	1.4	1.73463	1.765255	0.842	2.12320	2.1371	1.1019
	1.6	2.12374	2.182	0.651	2.68635	2.7218	0.81625
	1.8	3.02140	3.1536	0.427	3.95930	4.0723	0.5076

2. Test functions with a physical basis (circular/spherical tank). The experiments by Barkowiak *et al.* (1985) for a circular tank showed that the path lines of liquid particles for the lowest mode resemble the path lines due to an infinite-fluid horizontal dipole with singularity above the mean free surface at the tank's centreplane. If a Cartesian coordinate system Oyz has the origin at the intersection between the mean free surface and the tank's centreplane, a normalized dipole solution with singularity at $(0, a)$ is $\varphi_1 = R_0 y / (y^2 + (z - a)^2)$. The procedure can be generalized to a spherical tank with a cylindrical coordinate system $Or\theta z$. The horizontal dipole solutions are then either $\varphi_{1,1(\sin)} = R_0^2 r \sin \theta / (r^2 + (z - a)^2)^{3/2}$ or $\varphi_{1,1(\cos)} = R_0^2 r \cos \theta / (r^2 + (z - a)^2)^{3/2}$, $a > 0$. These test solutions satisfy Laplace equation and the volume conservation condition; the boundary conditions are in general not satisfied. The test functions are substituted into K_{Q_0, Σ_0} given by (1). The lowest eigenfrequency

¹ Presenting author

follows by minimizing K_{Q_0, Σ_0} with respect to a . Table 1 shows good agreement with benchmark numerical results and confirms that the estimate cannot be lower than the correct eigenfrequency (Table 1).

3. Analytical continuation is in some cases possible as part of procedures to estimate natural frequencies and modes. Chamfers (see, Figure 1a) and inclination of the tank bottom are examples. The natural modes φ'_n in a domain Q'_0 must be analytically continued into a domain Q_0 where an analytical solution φ_n exists. The objective is to express the natural frequencies $\sigma'_n = \sqrt{g\kappa'_n}$ for the domain Q'_0 in terms of the natural frequencies $\sigma_n = \sqrt{g\kappa_n}$ for the domain Q_0 with a small correcting factor that accounts for the difference in the liquid domains. Other assumptions are (i) the area/volume $Vol.(\delta Q_0)$ of the difference δQ_0 between the domains Q_0 and Q'_0 is small relative to the area/volume of Q_0 ; (ii) characteristic length dimensions of δQ_0 are small relative to the wavelengths associated with the natural modes φ'_n and φ_n ; (iii) the mean free surfaces Σ'_0 and Σ_0 of domains Q_0 and Q'_0 are the same. It follows by rewriting the variational equation (2) and asymptotic analysis that

$$\frac{\sigma_n'^2}{\sigma_n^2} = \frac{\kappa_n'}{\kappa_n} = 1 - \frac{\int_{\delta Q_0} (\nabla \varphi_n)^2 dQ}{\kappa_n \int_{\Sigma_0} (\varphi_n)^2 dS} + o\left(\frac{Vol.(\delta Q_0)}{Vol.(Q_0)}\right). \quad (3)$$

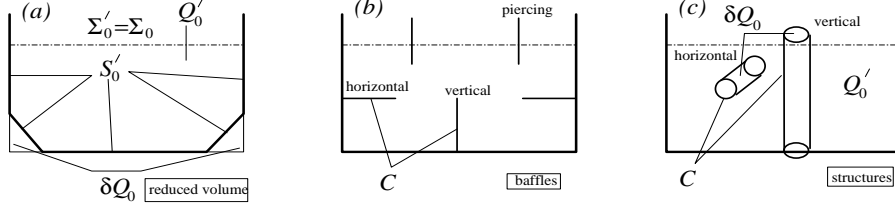


Figure 1. Examples of small reductions of rectangular tank. One can get explicit formulae (based on eq. (3)) for chamfered tanks, inclined bottom etc. Estimates for tanks with baffles (b) and poles (b) are based on eq. (4).

Analytical continuation **cannot** be used to estimate the effect of interior structures such as baffles, pump towers and screens on the natural frequencies (see, e.g. cases b and c in Figure 2). However, if the interior structures do not have a net source/sink effect on the flow and the cross-dimensions of the interior structure are small relative to both the main tank dimensions and the wavelength of the considered sloshing mode, the natural frequencies can be expressed in terms of the added mass coefficients and displaced mass of the interior structure. A similar procedure is possible for slender structures with small transverse cross-sections. The derivation starts with using Green's second identity in combination with the definition of added mass. The basic 3D formula is as follows

$$\frac{\sigma_m'^2}{\sigma_m^2} = \frac{\kappa_m'}{\kappa_m} = 1 - \frac{\sum_{j,k=1}^N \phi_{mj} \phi_{mk} [\delta_{kj} Vol.(\delta Q_0) + A_{jk} / \rho]}{\kappa_m \int_{\Sigma_0} \varphi_m^2 dS}, \quad \phi_{mj} = \left. \frac{\partial \varphi_m}{\partial x_j} \right|_P, \quad \phi_{mk} = \left. \frac{\partial \varphi_m}{\partial x_k} \right|_P; \quad (x_1, x_2, x_3) = (x, y, z). \quad (4)$$

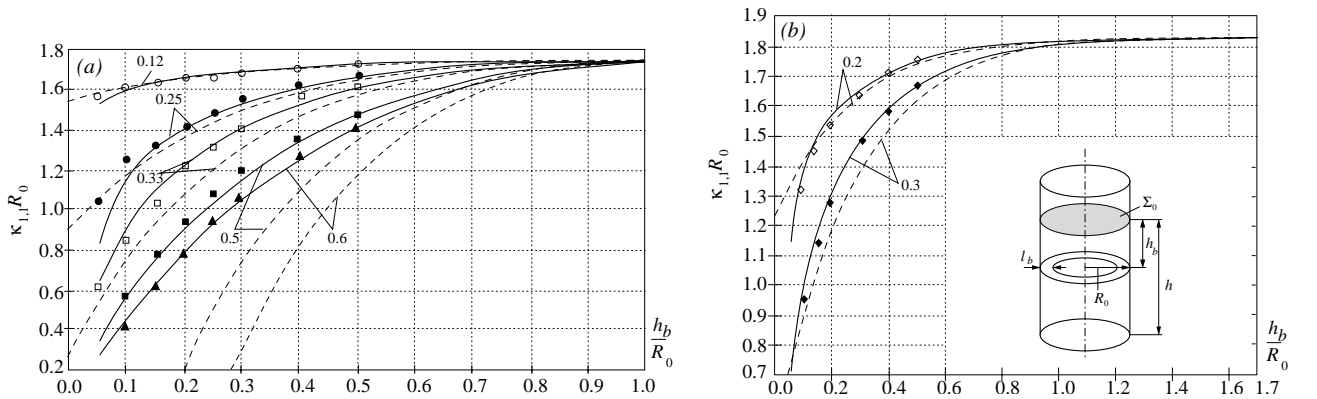


Figure 2. The non-dimensional lowest natural eigenvalue $\kappa_{1,1} R_0 = \sigma_{1,1}^2 R_0 / g$ versus the vertical location h_b of a ring baffle relative to the mean free surface in an upright circular cylindrical tank with radius R_0 . Dashed lines are drawn by using the asymptotic formula (3) by assuming $l_b / R_0 \ll 1$ and $h_b / l_b \geq O(1)$. Solid lines represent accurate numerical results. The numbers on the solid and dashed lines are values of l_b / R_0 . Points correspond to experimental data by Dorozhkin (pers.comm.) (case a, $h / R_0 = 1$) and Miskishev & Churilov (1977) (case b, $h / R_0 = 1.7$).

Here $\varphi_m \cos(\sigma_m t)$ is the velocity potential due to the m 'th eigenmode without the presence of the interior body. The formula expresses the effect of the change in the kinetic energy due to the interior structure. P

is either the geometrical centre of the internal body or the mounting point of a baffle and A_{ij} are frequency-independent added mass coefficients for the interior body. A close proximity of the tank boundaries and/or the free surface in terms of a rigid-wall condition must be accounted for in A_{ij} . Summation changes to $N = 2$ for two-dimensional problems. The formula can be generalized to include several interior bodies with possible hydrodynamic interaction.

Example of the use of the formula is represented in Figure 2. A slender-body formulation with 2D added mass coefficients with tank wall effects is used in accounting for the ring baffle in the vertical circular cylinder. The effects of the tank bottom and the free surface on the added mass are neglected. The asymptotic formula agrees well with accurate numerical results and experimental data. However, difficulties occur when the ring baffle comes too close to the free surface. Reasons are, for instance, local nonlinear free surface shallow-liquid effects and slamming. The formula has also been experimentally validated for a vertical pole in a rectangular tank.

4. Asymptotic methods. The mean free surface was assumed approximately the same when we related the eigenvalue problems for two tanks in the previous cases. This condition is, in general, not satisfied for the tapered tank in Figure 3a relative to a rectangular tank. In this case, one can employ an asymptotic method with the angle α defined in the figure as a small parameter. The focus is on waves along the Ox -axis. Due to the free-surface condition, the solution is presented as $\varphi(x, y, z) = \phi(x, y) \cosh(k_{i,0}(z + h))$ and $\sigma_{i,0}^2 / g = \kappa_{i,0} = k_{i,0} \tanh(k_{i,0}h)$, where ϕ and $k_{i,0}$ should be found from the corresponding boundary problem in the cross-sectional trapezoidal domain. Due to symmetry of the domain, the focus is on the half of the cross-section in Figure 3b. Because almost two-dimensional sloshing in the $x-z$ plane is considered, a small parameter δ is introduced to express the slow variation of the flow in the y -direction, i.e. $\phi(x, y) = f(x, \delta y) = f(x, y_1)$. Matching δ with α by using the wall boundary conditions gives $\delta^2 \sim \alpha$ and $\frac{\partial^2 f}{\partial x^2} + \frac{2\alpha}{L_2} \frac{\partial f}{\partial x} + k_{i,0}^2 f = 0$ for $y_1 = 0$ and $\partial f(x, 0) / \partial x = 0, x = \pm \frac{1}{2} L_1$. This is the spectral problem with respect to $f = f(x, 0)$ with the spectral parameter $k_{i,0}^2$. Its solution $k_{i,0}^2$ and the corresponding natural frequencies are given in the caption of Figure 3.

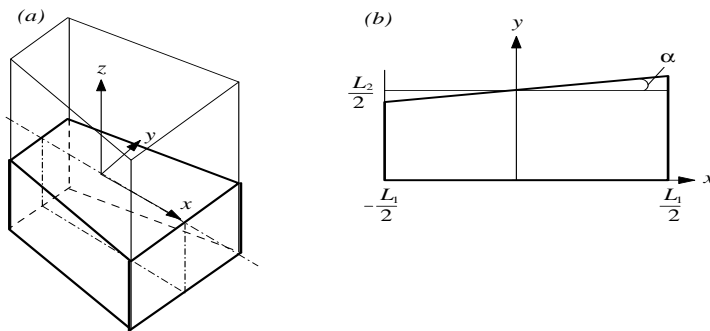


Figure 3. 3D dimensional and top view of one half part of a trapezoidal-base tank. The analytical solution for a 3D rectangular tank is used as the zero-order approximation for small α . The result for the natural frequencies corresponding to longitudinal standing waves along the Ox -axis is $\sigma_{i,0}^2 / g = k_{i,0} \tanh(k_{i,0}h)$ with $k_{i,0}^2 = (\pi i / L_1)^2 + (\alpha / L_2)^2$.

5. A linear modal method transforms the sloshing problem to a system of ordinary differential equations coupling the generalised coordinates $\beta_i(t)$ representing the wave elevations of the natural sloshing modes. The equations are $\ddot{\beta}_m + \sigma_m^2 \beta_m = K_m(t)$, $m = 1, 2, \dots$, where σ_m are natural sloshing frequencies and $K_m(t) = -\lambda_{1m} \mu_m^{-1} (\ddot{\eta}_1(t) - g\eta_5(t)) - \lambda_{2m} \mu_m^{-1} (\ddot{\eta}_2(t) + g\eta_4(t)) - \sum_{k=4}^6 \ddot{\eta}_k(t) \lambda_{0(k-3)m} \mu_m^{-1}$. Here $\eta_i(t)$ are the translatory and angular motions of the tank and the hydrodynamic coefficients $\lambda_{1m}, \lambda_{2m}, \mu_m$ and $\lambda_{0im}, i = 1, 2, 3$ are related to quadratures over the natural sloshing modes and the so-called Stokes-Joukowski potential. Damping terms due to, for instance, viscous boundary-layer effects may be added. Moreover, there exist the so-called Lukovsky formulae that express the hydrodynamic force and moment in terms of $\eta_i(t)$ and the generalised coordinates with the same hydrodynamic coefficients and the inertia tensor computed as quadrature over the Stokes-Joukowski potential (Faltinsen & Timokha, 2009).

Example 1. Using the dipole solution from 2., one can construct a one-dimensional modal equation (only the lowest mode matters) for transient sloshing during a transverse maneuver of a circular tank as illustrated in Figure 4a. The horizontal hydrodynamic force is considered Figure 4b.

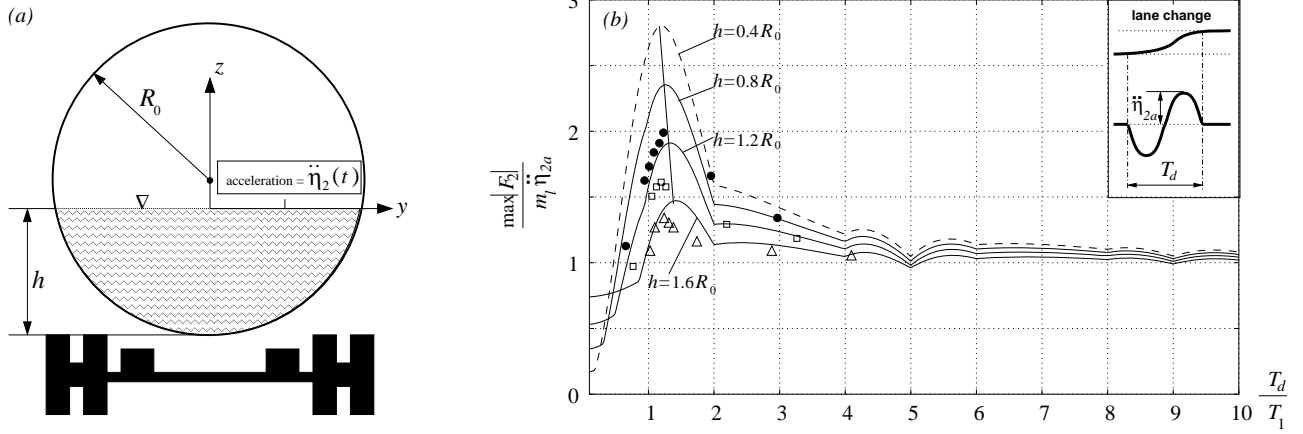


Figure 4. Simulation of lane change of a tank vehicle with a circular cylindrical tank. The transverse acceleration of the vehicle is $\ddot{\eta}_2(t)$. The maximum horizontal hydrodynamic force $\max |F_2|$ divided by the maximum horizontal frozen liquid force $m_l \ddot{\eta}_{2a}$ is presented as a function of the ratio between the duration T_d of the manoeuvre and the highest natural sloshing period T_1 for different liquid depth-to-cylinder ratios h/R_0 . The lane-change acceleration is idealized as a sinusoidal function of time (see, part b). Along with linear theoretical prediction by the two-mode model (solid and dashed lines), part (b) presents numerical results by Moderassi-Tehrani et al. (2006) obtained by using the commercial CFD-code FLUENT. FLUENT data correspond to $h/R_0 = 0.8$ (\bullet), 1.2 (\square) and 1.6 (Δ).

Example 2. The hydrodynamic forces and moments are functions of the hydrodynamic coefficients of the modal method. The corresponding frequency-domain added mass coefficients are frequency dependent with either positive or negative values and are infinite when the forcing frequency $\sigma = \sigma_n$ (n is a fixed number of the natural mode). The singular behavior is $O[(\sigma - \sigma_n)^{-1}]$ as $\sigma \rightarrow \sigma_n$. Even though the product of two added mass coefficients is $O[(\sigma - \sigma_n)^{-2}]$ as $\sigma \rightarrow \sigma_n$, combinations of products of the added mass coefficients may lead to a singular behaviour $O[(\sigma - \sigma_n)^{-1}]$ as $\sigma \rightarrow \sigma_n$. Newman (pers. comm.) showed by simulations (and derivations for a rectangular tank) that the singularity of $A_{44}A_{22} - A_{24}^2$ is $O[(\sigma - \sigma_n)^{-1}]$. Here A_{22}, A_{24} and A_{44} are the tank's added mass coefficients in sway, coupled sway-roll and roll, respectively. This fact was essential when Newman explained why the coupled sway and roll of a hemispheroid in regular beam sea waves are finite at the resonance frequency of sloshing. Using the modal-based expressions for added mass coefficients makes this point straightforward to explain in general. Indeed, the primary singular terms of the added mass at $\sigma = \sigma_n$ are

$$A_{44} = \frac{1}{\mu_n} \left(-\frac{g\lambda_{2n}}{\sigma^2} + \lambda_{01n} \right)^2 \frac{\sigma^2}{\sigma_n^2 - \sigma^2}; \quad A_{22} = \frac{\lambda_{2n}^2}{\mu_n} \frac{\sigma^2}{\sigma_n^2 - \sigma^2}; \quad A_{24} = \frac{\lambda_{2n}}{\mu_n} \left(-\frac{g\lambda_{2n}}{\sigma^2} + \lambda_{01n} \right) \frac{\sigma^2}{\sigma_n^2 - \sigma^2}.$$

These terms annihilate when we consider $A_{44}A_{22} - A_{24}^2$. This fact applies for any 2D and 3D tank.

Barkowiak, K., Gampert, B. and Siekmann, J. (1985) On liquid motion in a circular cylinder with horizontal axis. *Acta Mechanica* 54, 207-220.

Faltinsen, O.M., Timokha, A.N. (2009) *Sloshing*. Cambridge University Press.

Feschenko, S.F., Lukovsky, I.A., Rabinovich, B.I. and Dokuchaev, L.V. (1969) *Methods for Determining Added Fluid Mass in Mobile Cavities*. Kiev: Naukova dumka (in Russian).

McIver, P. (1989) Sloshing frequencies for cylindrical and spherical containers filled to an arbitrary depth. *Journal of Fluid Mechanics* 201, 243-257.

Mikishev, G.N. and Churilov, G.A. (1977) Some results on experimental hydrodynamic coefficients for a cylinder with ribs. In book: *Oscillations of Elastic Constructions with Liquid*. Tomsk: Tomsk University, p. 31-37 (in Russian).

Moderassi-Tehrani, K., Rakheja, S. and Sedaghati, R. (2006) Analysis of the overturning moment caused by transient liquid slosh inside a partly filled moving tank. *Proc. IMechE, Part D: J. Automobile Engineering* 220, 289-301.